

EXTENSION OF THE NIST TRISTIMULUS COLORIMETER FOR SOLID-STATE LIGHT SOURCE MEASUREMENTS

G. P. Eppeldauer¹, Zs. Kosztian², J. D. Schanda², G. Schanda³, C. C. Miller¹,
T. C. Larason¹, and Y. Ohno¹

¹National Institute of Standards and Technology, USA

²University of Pannonia, Hungary

³TENZI, Hungary

ABSTRACT

In order to obtain improved color measurement uncertainties for solid-state light (SSL) sources, the second generation tristimulus colorimeter of NIST has been extended with a fifth channel to perform efficient matrix corrections for the spectral mismatch of the realized channels. It is described how the tristimulus values can be determined using detector-based calibration and matrix corrections. Using modelling, the accuracy of the spectral mismatch corrections from both the detector-based calibration and the matrix corrections is compared.

Keywords: colorimetry, matrix correction, spectral mismatch, responsivity, tristimulus

1. INTRODUCTION

Tristimulus colorimeters calibrated with detector standards [1, 2] can have equal or better performance than source-standard calibrated spectral colorimeters. However, in either system, the uncertainty of solid-state light (SSL) source measurements can be high, due to stray light errors and bandpass errors with monochromator-based colorimeters and due to spectral mismatch in the realized channels for tristimulus colorimeters. The spectral mismatch errors must be corrected effectively in the wavelength range where the SSL sources emit light to perform accurate color measurements. The matrix correction method introduced with analog electronic circuits in 1976 [3] is utilized in this work.

2. NEW GENERATION COLORIMETER

Since the first generation tristimulus colorimeter of NIST had a long-term responsivity degradation (caused by the open Si photodiodes in the applied trap-detector) and

also a light leakage around the filters (because the baffling at the input of the trap-detector was not efficient), a second generation colorimeter was developed. The detector is a large-area single-element silicon photodiode closed with a wedge window. The 0.5° wedge was needed to avoid interference fringes in the output signal of the photodiode when calibrated at the tunable-laser based facility. The separations on the two sides of the temperature controlled filter-wheel are small resulting in five orders of magnitude blocking in the blue and IR wavelength ranges even in the input aperture is overfilled by the incident light. Also, the thickness of the filter packages was at least 4.5 mm to minimize fringes. The picture of the second generation colorimeter is shown in Fig. 1. The front cover, including a 5 mm diameter aperture was removed for better illustration.



Figure 1. Picture of the single-element Si photodiode based colorimeter.

A preamplifier with eight decade gain selection is attached to the side of the colorimeter. The filter combinations were individually optimized to obtain the smallest possible spectral mismatch to the CIE standard color matching functions. The measured spectral responsivity functions of the colorimeter channels are shown on a loga-

rithmic scale in Fig. 2. The relative expanded uncertainty of the spectral responsivity measurements was 0.1 % ($k=2$). No responsivity degradation could be measured on this colorimeter between 2007 and 2009.

3. TRISTIMULUS VALUES CALCULATION

3.1. Detector-based method

First, the tristimulus values were determined by calculating the detector-based calibration factors. Each calibration factor is a ratio where the numerator is the CIE tristimulus value and the denominator is the output signal (photocurrent) of the channel:

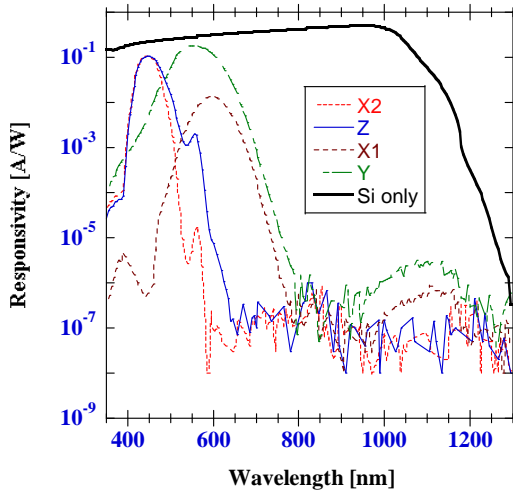


Figure 2. Measured spectral responsivity of the colorimeter channels.

$$\begin{aligned}
 k_{X_1} &= \frac{X_1}{I_{X_1}} = \frac{K_m \int_{\lambda} E(\lambda) \bar{x}_1(\lambda) d\lambda}{\int_{\lambda} E(\lambda) s_{X_1}(\lambda) d\lambda} \\
 k_{X_2} &= \frac{X_2}{I_{X_2}} = \frac{K_m \int_{\lambda} E(\lambda) \bar{x}_2(\lambda) d\lambda}{\int_{\lambda} E(\lambda) s_{X_2}(\lambda) d\lambda} \\
 k_Y &= \frac{Y}{I_Y} = \frac{K_m \int_{\lambda} E(\lambda) V(\lambda) d\lambda}{\int_{\lambda} E(\lambda) s_Y(\lambda) d\lambda} \\
 k_Z &= \frac{Z}{I_Z} = \frac{K_m \int_{\lambda} E(\lambda) \bar{z}(\lambda) d\lambda}{\int_{\lambda} E(\lambda) s_Z(\lambda) d\lambda}
 \end{aligned} \quad (1)$$

where $E(\lambda)$ is the relative spectral distribution of the reference source (not a standard in this calibration), $\bar{x}_1(\lambda)$, $\bar{x}_2(\lambda)$, $V(\lambda)$, and $\bar{z}(\lambda)$ are the CIE color matching functions, K_m is the maximum spectral luminous efficacy, 683 lm/W, $s_{X_1}(\lambda)$, $s_{X_2}(\lambda)$, $s_Y(\lambda)$, and $s_Z(\lambda)$ are the measured spectral responsivi-

ties of the realized channels (as shown in Fig. 2), and λ is the wavelength. Each ratio performs spectral mismatch correction and amplitude correction for one of the realized channels. These calibration factors are used to multiply the channel output currents when a test light source is measured to obtain the tristimulus values of that test light source.

3.2. Matrix correction method

The second method to determine the tristimulus values is performed using matrix transformation. In this case, instead of the integral ratios in Eq. 1, a matrix correction is used to correct for the spectral mismatch errors of the realized channels. The basic equation of the applied matrix transformation for the realized four channels (without showing the modified channel calibration factors) is:

$$\begin{bmatrix} X_T \\ Y_T \\ Z_T \end{bmatrix} = \begin{bmatrix} a_{11} & a_{21} & a_{31} & a_{41} \\ a_{12} & a_{22} & a_{32} & a_{42} \\ a_{13} & a_{23} & a_{33} & a_{43} \end{bmatrix} \cdot \begin{bmatrix} I_{X_1} \\ I_{X_2} \\ I_Y \\ I_Z \end{bmatrix} \quad (2)$$

where I_{X_1} , I_{X_2} , I_Y , and I_Z are the channel output currents, a_{11} to a_{43} are the elements of the 3 x 4 correction matrix, X_T , Y_T , and Z_T are the matrix corrected tristimulus values of a test light source. In order to perform the matrix correction, the measured I output currents are converted into digital numbers that can be corrected by the calculated software matrix. The matrix optimization is similar to the optimization of the filter combinations.

In order to better correct the missing or excess responsivity components of the realized channels, an additional fifth channel was added to the colorimeter. The I output-currents of the channels are multiplied by the K modified calibration factors derived from Eq. (1). The modification was made by tuning the integral ratios (the spectral mismatch correction factors) to unity and adding the gain corrections:

$$\begin{bmatrix} X_T \\ Y_T \\ Z_T \end{bmatrix} = \begin{bmatrix} a_{11} & a_{21} & a_{31} & a_{41} & a_{51} \\ a_{12} & a_{22} & a_{32} & a_{42} & a_{52} \\ a_{13} & a_{23} & a_{33} & a_{43} & a_{53} \end{bmatrix} \cdot \begin{bmatrix} I_{X_1} * k_{X_1}' \\ I_{X_2} * k_{X_2}' \\ I_Y * k_Y' \\ I_Z * k_Z' \\ I_K \end{bmatrix} \quad (3)$$

Because of the added fifth (K) channel, a 3 x 5 correction matrix is used. The K chan-

nel produces signals at wavelength intervals where the test sources emit light and the spectral mismatch errors of the realized channels are significant. The spectral responsivity of the K channel was calculated from a large number of spectral power distributions such as Planckian from 2000 K to 5100 K, 5 white LEDs, 28 blue LEDs, 7 green LEDs, 21 red LEDs, CIE D65 and an equi-energy distribution. The realized function approximates a Gaussian distribution [4]. The spectral responsivities of the realized five channels are shown on a linear scale in Fig. 3. The K channel is also shown separately on a logarithmic scale in Fig. 4. It can be seen that the useful spectral coverage ends at about 600 nm. This means that the matrix correction cannot be efficient enough for red LEDs that emit light at wavelengths longer than 600 nm.

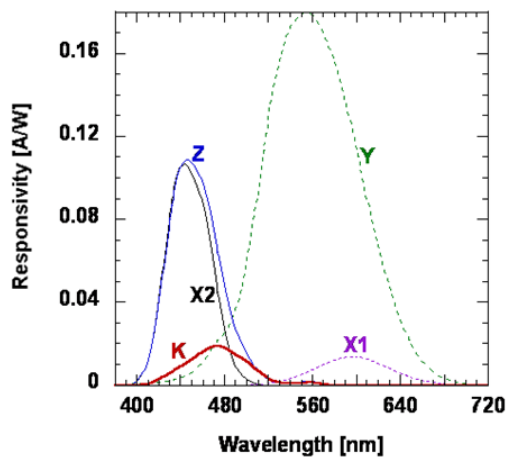


Figure 3. Spectral responsivity of the five realized channels on a linear scale.

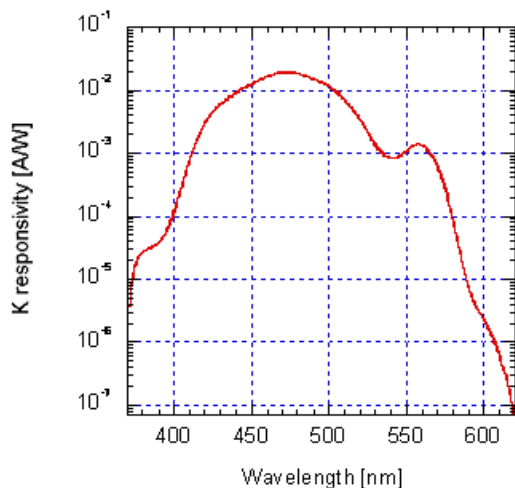


Figure 4. Spectral responsivity of the K correction channel on a logarithmic Y-scale.

4. COLORIMETER EXTENSION

The analog output voltages of the colorimeter channels were converted into digital numbers using a 16 bit analog-to-digital converter. A user interface screen-image was developed where the output voltage of the selected channel is continuously displayed. Measurements can be taken at different channel and gain-range selections. The gain calibration factors for the different gain selections are used to calculate the I output currents. The number of measurements can be selected and then displayed to obtain the mean value and the standard deviation for the measured data of the channel outputs. The screen-image was used to measure the tristimulus values and the chromaticity coordinates either with or without matrix corrections.

For detector-based calibrations, where the matrix corrections are not used, four reference source distributions can be selected to determine the calibration factors using Eq. 1: Illuminant A, equi-energy, D65, and a user defined distribution. The color correction factors are included in the channel calibration factors which are stored in a file of the colorimeter software. The illuminance responsivity of the Y channel is also stored using the three reference source distributions. Also, the optimal multipliers for the matrix elements are stored. These multipliers are optimized such that multiplying the five output-currents with them and then either subtracting or adding the product to the three output channels, the corrected tristimulus values will be obtained with the smallest errors relative to the CIE standard color-matching functions. The multipliers depend on the six source distributions that can be selected for matrix corrections. The values in the stored files can be changed or replaced at detector-based re-calibrations.

The need for matrix correction can be selected on the user interface screen-image. Different matrix corrections can be selected for Planck sources, blue LEDs, green LEDs, red LEDs, white LEDs, and for all of these sources. The measured data are displayed (including the X, Y, Z, x, y, and lux values) with and without matrix corrections.

5. COLORIMETER EVALUATION

The extended colorimeter was tested using simulations. The simulations included

the chromaticity calculation of several source distributions. The real chromaticity values were calculated from the spectral products of monochromator measured (or Planckian) source distributions and the CIE standard 2° color matching functions. The modelled chromaticity values from the calculated out-put current of the channels (which is equal to the spectral product of the measured or Planckian source distribution and the realized and measured channel spectral responsivities) were compared to the real chromaticity values. Also, the matrix corrected chromaticity values were calculated and compared to the real values.

The chromaticity differences were calculated for the different corrections (modelled colors) relative to the real colors. Table 1 shows the average $\Delta(u',v')$ values obtained with detector-based calibration (without matrix correction). The color differences were small and similar to each other when Planckian sources were modelled using the three reference source distributions in Eq. 1. However, the color differences were about twenty times larger when LEDs were measured.

Table 1. Average $\Delta(u',v') \times 1000$ from detector-based calibration (without matrix use).

| Optimized for: | CIE std. Illum. A | CIE std. Illum. D65 | Equi-energy Illum. |
|----------------|-------------------|---------------------|--------------------|
| Planck sources | 0.28 | 0.29 | 0.28 |
| LEDs | 5.84 | 5.56 | 5.69 |

Table 2 shows the average and maximum $\Delta(u',v')$ values obtained for the five test sources in the first column when using the different matrix selections shown in the first line of Table 2. It is shown, that the average chromaticity differences can be small if the proper matrix correction is selected for a given test source. It also can be seen that using the "All" matrix selection, the LED chromaticity differences were improved by about an order of magnitude compared to the chromaticity differences obtained with the detector-based calibration (without matrix correction). The improvement for the red LEDs was less because the wavelength coverage of the K channel was limited to about 600 nm. As shown, large errors can be obtained if not the proper matrix is selected.

6. CONCLUSIONS

A new generation tristimulus colorimeter has been developed at NIST which has been calibrated against detector standards. In order to measure SSL-sources with low colorimetric uncertainty, the colorimeter has been extended with a fifth channel, an analog-to-digital converter, and a software to perform improved spectral mismatch corrections using matrixes optimized for six different test-source distributions. When matrix corrections were used with the detector-based calibration, the spectral mismatch corrections could be significantly improved for SSL sources including LEDs. The average modeled chromaticity differences (referenced to the real chromaticity values) were more than twenty times smaller with the applied matrix corrections.

Table 2. $\Delta(u',v') \times 1000$ of five test sources

| Matrix used for sources: | All | | Planckian | | red LEDs | | green LEDs | | blue LEDs | | white LEDs | |
|--------------------------|------|-------|-----------|------|----------|------|------------|------|-----------|------|------------|------|
| | Ave | Max | Ave | Max | Ave | Max | Ave | Max | Ave | Max | Ave | Max |
| incand. sources | 0.36 | 1.54 | 0.01 | 0.12 | 252 | 301 | 22 | 28 | 41 | 54 | 0.71 | 1.00 |
| red LEDs | 6.00 | 26.34 | 12 | 21 | 0.66 | 7.16 | 81 | 112 | 85.5 | 138 | 7.61 | 18 |
| green LEDs | 0.38 | 0.88 | 10 | 17 | 701 | 1186 | 0.04 | 0.16 | 43 | 55 | 5.94 | 8.5 |
| blue LEDs | 0.61 | 2.42 | 30 | 39 | 473 | 525 | 89 | 147 | 0.23 | 1.31 | 7.77 | 9.76 |
| white LEDs | 0.64 | 0.95 | 1.6 | 2.57 | 224 | 306 | 26 | 31 | 37 | 59 | 0.31 | 1.37 |

REFERENCES

1. G. Eppeldauer, Spectral Response Based Calibration Method of Tristimulus Colorimeters, J. Res. Natl. Inst. Stand. Technol. Vol. 103, No. 6. p. 615, 1998.
2. G. P. Eppeldauer, Editor, Optical radiation measurements based on detector standards, NIST Technical Note #1621, Printing and Duplicating, National Institute of Standards and Technology, March, 2009.
3. G. Eppeldauer and J. Schanda, Colorimeter with matrix transformation, AIC Conference on Colour Dynamics '76, p. 403-413, Budapest, June 8-11, 1976.
4. Zs. Kosztyan, S. Sturm, D. Muller, J. Schanda, Decreasing colour measuring systematic error in image taking tristimulus colorimeters, Proc. CIE Expert Symposium on Advances in Photometry and Colorimetry, p. 21-25, CIE Central Bureau, 2008.

Authors

G. P. Eppeldauer, Zs. Kosztyan, J. D. Schanda,
G. Schanda, C. C. Miller, T. C. Larason, and Y.
Ohno
Contact address:
National Institute of Standards and Technology
100 Bureau Drive
Gaithersburg, Maryland 20899, USA
Phone: 301-975-2338, FAX: 301-869-5700,
Email: george.eppeldauer @nist.gov